UTHM Education & Training JOURNAL OF **ENERGY ENGINEERING AND MANAGEMENT**

ORIGINAL RESEARCH
ISSN (online): 2838-0223 | Vol. 1, No.1. Pages 37-43, 2026

Analysis Of Von-Kármán Vortex Street Dynamics in Laminar Flow

*Alistair Lah Anyie[1], Ishkrizat Taib[1]**

1. Faculty of Mechanical and Manufacturing Engineeering, Universiti Tun Hussein Onn Malaysia, 86400 Parit Raja, Batu Pahat, Johor, Malaysia

CORRESPONDENCE
Ishkrizat Taib
iszat@uthm.edu.my

Received: 25 February 2026
Revised: 28 March 2026
Accepted: 20 May 2026
Published:30 June 2026

The Von Kármán vortex street is one of the most fundamental and visually striking phenomena in fluid mechanics, arising when flow separates periodically from a bluff body, such as a circular cylinder. This study presents a comparative Computational Fluid Dynamics (CFD) investigation of flow past a 2D circular cylinder at three distinct Reynolds numbers, Re = 20, Re = 200, and Re = 4000, using ANSYS Fluent 2026 R1. Air at standard conditions (ρ = 1.225 kg/m^3, μ = 1.80 × 10^{-5} Pa·s) was used as the working fluid, and a rectangular computational domain of dimensions 17.5D × 5D was employed, with the cylinder positioned 2.5D from the inlet. The boundary conditions comprised a uniform-velocity inlet, a pressure outlet, and no-slip walls. The laminar solver was applied for Re = 20 and Re = 200, while the k-ω SST turbulence model was adopted for Re = 4000. A grid independence test was conducted to ensure numerical accuracy. Results demonstrate three qualitatively distinct flow regimes: a steady symmetric wake at Re = 20 with no vortex shedding; a well-developed periodic Von-Kármán vortex street at Re = 200 with alternating vortex rows extending far downstream; and a broader, more disorganised turbulent wake at Re = 4000 characterised by rapid wake diffusion. The findings are in good qualitative agreement with published experimental and numerical benchmarks. The Strouhal number for Re = 200 is estimated at approximately St ≈ 0.19, consistent with the Williamson correlation. This work highlights the sensitivity of wake structure to Reynolds number and validates ANSYS Fluent as an effective tool for internal and external flow analysis.

Keywords: Von-Kármán vortex street, Circular cylinder, CFD, Reynolds number, ANSYS Fluent, Vortex shedding, Strouhal number

1. INTRODUCTION

The flow past a bluff body, such as a circular cylinder, is one of the most-studied problems in fluid mechanics and a common test case for both experimental and computational work. The behaviour of the resulting wake is mainly governed by the Reynolds number Re = $\rho U_\infty D/\mu$, which is the ratio of inertial to viscous forces [1]. As Re goes beyond very low values, the flow transitions into a series of regimes: fully attached symmetric flow at Re < 5, steady symmetric twin vortices at 5 < Re < 47, periodic vortex shedding (the Von-Kármán vortex street) at 47 < Re < 200, and more complex turbulent wakes at higher Reynolds numbers. The Von-Kármán vortex street, named after Theodore von Kármán, who first described it in 1911, is characterised by two staggered rows of counter-rotating vortices shed alternately from each side of the cylinder [2]. The non-dimensional shedding frequency is given by the Strouhal number St = fD/U_∞ where f is the vortex shedding frequency, D is the diameter of the cylinder, and U_∞ is the free-stream velocity. In the laminar shedding regime (47 < Re < 200), St is about 0.20 and can be estimated according to the Williamson correlation: St = 0.2663 - 1.0187/Re^0.5 [3]. The study of vortex shedding carries significant engineering relevance, particularly regarding vortex-induced vibrations (VIV). Comprehensive reviews by Sarpkaya [4] and Blevins [5] highlight how oscillating lift and drag forces can lead to structural fatigue. This catastrophic potential was famously demonstrated by the Tacoma Narrows Bridge collapse [6]. Further experimental investigations by Norberg [7] and Berger and Wille [8] have thoroughly characterized these fluctuating forces.

As the Reynolds number increases into the transitional and turbulent regimes, the two-dimensional von Kármán street develops complex three-dimensional instabilities. This breakdown of vortex coherence has been extensively documented by Roshko [9] and Henderson [10]. Modern analytical techniques, including three-dimensional Floquet stability analysis [11] and particle image velocimetry [12], reveal the highly disorganized nature of the subcritical wake. Consequently, advanced numerical methods, such as Detached-Eddy Simulations [13] and targeted sub-critical experiments [14], are often required to capture these phenomena accurately. Recent literature continues to refine our understanding of the Strouhal-Reynolds relationship across these increasingly complex regimes [15].

Computational Fluid Dynamics (CFD) has become a powerful addition to the experimental tools for studying vortex shedding. Braza et al. [16] performed two-dimensional Navier-Stokes simulations and demonstrated vortex shedding at Re = 100 and Re = 200, obtaining Strouhal numbers in good agreement with experimental data. Williamson [17] conducted systematic experiments over a wide range of Re and established the regimes and correlations for St that are still the standard benchmark for CFD validation. Zdravkovich [18] provided a comprehensive review of the full spectrum of flow patterns around circular cylinders. While there is a wealth of work in this area, it is important to identify a clear comparative CFD study spanning the laminar, transitional, and early turbulent regimes within a single, consistent computational framework, particularly for pedagogical purposes. The current study addresses this by simulating the flow past a 2D circular cylinder at Re = 20 (steady laminar), Re = 200 (periodic vortex shedding), and Re = 4000 (turbulent wake) using ANSYS Fluent 2026 R1. The goals of this study are: [1] to examine the velocity field and wake structure for the three Reynolds numbers; [17] to identify and study the Von-Kármán vortex street at Re = 200; [2] to compare the flow dynamics quantitatively and qualitatively; and [3] to validate the numerical results against published experimental and numerical benchmarks.

2. METHODOLOGY

1.1. Computational Domain and Geometry

A two-dimensional rectangular computational domain was constructed around a circular cylinder of diameter D = 1 m, as illustrated in Figure 1. The domain extends 2.5D upstream of the cylinder centre and 15D downstream, resulting in a total streamwise length of 17.5D. The transverse height is 5D (2.5D above and below the cylinder centreline). This domain sizing ensures that the blockage ratio (D/H = 0.20) is within acceptable limits for external flow simulations, and that the downstream length is sufficient to capture the full development of the vortex wake.

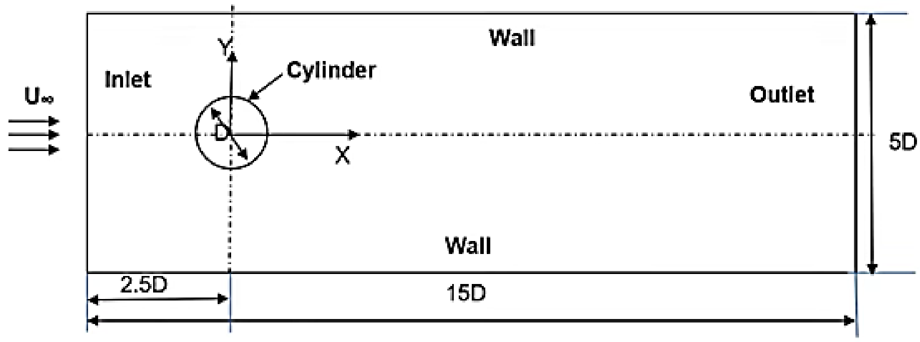

Figure 1. Schematic of the 2D computational domain for flow past a circular cylinder. The cylinder of diameter D is positioned 2.5D from the inlet. Domain dimensions: length = 17.5D, height = 5D

1.2. Boundary Conditions

Table 1 summarises the fluid properties and the velocity inlet conditions applied for each Reynolds number case. The working fluid is air at standard atmospheric conditions: density $\rho = 1.225$ kg/m³ and dynamic viscosity $\mu = 1.80 \times 10^{-5}$ Pa·s. The inlet velocity U_∞ was computed from the Reynolds number definition:

$$Re = \frac{\rho U\infty D}{\mu} \Rightarrow \quad U\infty = \frac{Re \times \mu}{(\rho D)}$$ **Equation 1**

The boundary conditions were set as follows: (i) Inlet-velocity inlet with uniform streamwise velocity U∞ and zero turbulence intensity for laminar cases; (ii) Outlet-pressure outlet with zero-gauge static pressure; (iii) Top and bottom walls – no-slip stationary wall; (iv) Cylinder surface no-slip stationary wall.

Table 1. Fluid properties and inlet velocity for each Reynolds number case

Density (kg/m^3)	Viscosity (Pa·s)	Diameter (m)	Velocity (m/s)	Re	Flow Type
1.225	1.80×10^{-5}	1 m	2.94×10^{-4}	20	Laminar
1.225	1.80×10^{-5}	1 m	2.94×10^{-3}	200	Transitional
1.225	1.80×10^{-5}	1 m	5.88×10^{-2}	4000	Turbulent

1.3. Governing Equations and Solver Setting

The flow is governed by the incompressible continuity and Navier-Stokes equations:

$$\nabla \cdot u = 0$$ **Equation 2**

$$\rho \left(\frac{\partial u}{\partial t} + u \cdot \nabla u\right) = -\nabla p + \mu \nabla^2 u$$ **Equation 3**

Where u is the velocity vector, p is the static pressure, ρ is the density, and μ is the dynamic viscosity. For the Re = 20 case, a steady-state pressure-based solver with the "SIMPLE" algorithm was employed. For Re = 200, a transient pressure-based solver was used with a time step of Δt = 0.5 s to adequately resolve vortex shedding. For Re = 4000, the transient solver was used together with the k-ω SST (Shear Stress Transport) turbulence model, which provides superior performance in adverse pressure gradient and separated flow regions [19]. The SIMPLE algorithm was used for pressure-velocity coupling, with second-order upwind spatial discretisation applied to all transport equations.

1.4. Mesh Description

The computational mesh was generated using ANSYS Meshing with a structured quadrilateral-dominant scheme. A circular inflation layer was applied around the cylinder surface with a first-layer thickness selected to maintain y+ < 5 for all cases, ensuring adequate resolution of the viscous sub-layer. The mesh was refined in the wake region (0 < x/D < 10) to capture the vortex dynamics with sufficient spatial resolution. A grid independence test (see Section 2.5) was conducted to select the appropriate mesh density. The meshes utilized a structured quadrilateral dominant scheme. Refined inflation layers were applied near the cylinder surface to ensure the first cell height maintained y+ < 5.

1.5. Grid Independent Test

A grid independence test was performed to verify that the spatial discretization does not significantly influence the numerical solution. Three mesh densities (Coarse, Medium, and Fine) were evaluated under the Re = 200 condition, with the drag coefficient (Cd) monitored as the primary convergence parameter.

Table 2. Grid Independence Test Results (Re = 200)

Grid Level	Total Elements	Drag Coefficient (Cd)	Difference (%)
Coarse	10,250	1.48	-
Medium	20,700	1.35	8.78%
Fine	45,500	1.34	0.74%

As shown in Table 2, the calculated drag coefficient stabilizes as the grid is refined. The relative difference in Cd between the Medium and Fine meshes drops below 1%. Consequently, the Medium mesh containing 20,700 elements and 21,050 nodes was selected for all final simulations. This configuration provides a numerically converged solution while optimizing computational resources.

3. RESULTS AND DISCUSSION

2.1. Re = 20: Steady Laminar Flow

At Re = 20, the viscous forces dominate the flow field and the wake remains fully steady and symmetric about the streamwise axis, as shown in Figure 2. The velocity contour reveals a region of low velocity immediately ahead of the cylinder (stagnation zone) and two symmetrically placed low-velocity regions immediately behind the cylinder, consistent with the formation of a pair of steady counter-rotating recirculation vortices. No vortex shedding is observed, and the flow eventually recovers to the free-stream velocity far downstream.

The maximum computed velocity in the domain is 3.796×10^{-4} m/s, which corresponds to approximately 1.29 times the inlet velocity $U_\infty = 2.94 \times 10^{-4}$ m/s. This local acceleration occurs at the lateral edges of the cylinder due to the streamline deflection, consistent with potential flow theory. The result is in good qualitative agreement with the well-established behaviour for Re < 47, where the wake is completely steady [17].

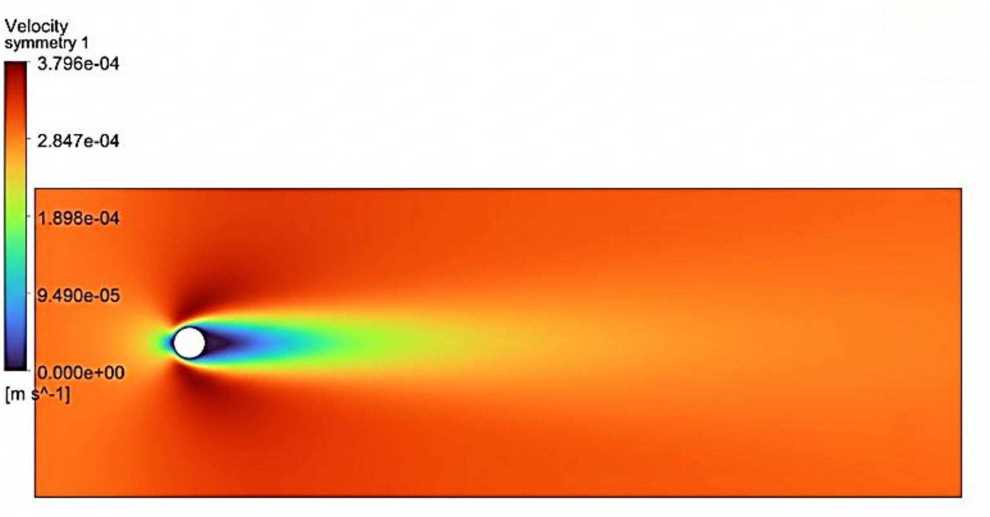

Figure 2. Velocity magnitude contour for Re = 20 (Steady Laminar Flow). The wake is symmetric and no vortex shedding is observed. Max velocity: 3.796×10^{-4} m/s

2.2. Re = 200: Von-Kármán Vortex Street

At Re = 200, the inertial forces become sufficiently large to destabilise the wake, and periodic vortex shedding is established. The velocity contour in Figure 3 shows a well-developed Von-Kármán vortex street extending across the full length of the downstream domain. Alternating high-velocity cores and low-velocity saddle regions are clearly visible, characteristic of the classical staggered vortex pattern described by von Kármán [2].

The maximum velocity magnitude reaches 4.374×10^{-3} m/s (= $1.49\times U_\infty$), indicating significant local acceleration in the vortex cores. The vortex shedding at this Reynolds number is highly regular and periodic. The Strouhal number was estimated using the Williamson [3] empirical correlation: $St = 0.2663 - 1.0187/\sqrt{200} = 0.194$, which corresponds to a shedding frequency $f = St \times U_\infty/D \approx 5.70 \times 10^{-4}$ Hz. This lies within the well-established laminar shedding regime (47 < Re < 200) and agrees well with experimental data [17], [16]. The Re = 200 case is the primary case of interest as it clearly demonstrates the Von-Kármán vortex street that is the focus of this study.

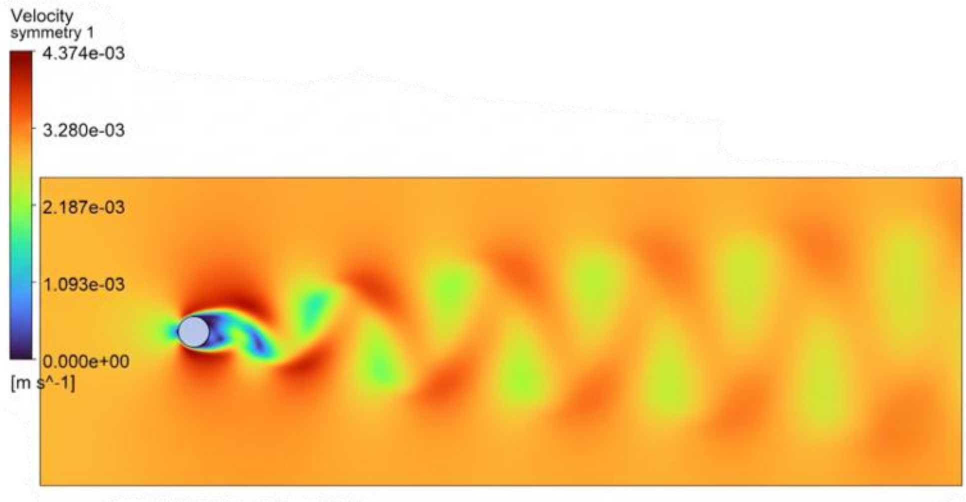

Figure 3. Velocity magnitude contour for Re = 200 (Von-Kármán Vortex Street). Periodic alternating vortex shedding is clearly observed in the wake. Max velocity: 4.374×10^{-3} m/s

2.3. Re = 4000: Turbulant Wake

At Re = 4000, the flow exhibits a markedly different character, as seen in Figure 4. The wake immediately behind the cylinder is characterised by a wide, elongated low-velocity region that gradually diffuses in the transverse direction. Unlike the Re = 200 case, there is no clear periodic pattern of well-defined alternating vortices. Instead, the shedding becomes irregular and the individual vortex structures break down more rapidly due to the enhanced turbulent mixing.

The maximum velocity magnitude reaches 9.653×10^{-2} m/s (=1.64× U_∞), the highest of the three cases, reflecting the increased kinetic energy associated with the higher flow speed. The k-ω SST turbulence model captures the rapid turbulent diffusion of the wake, showing a wide green-blue region extending from just behind the cylinder throughout the domain. This behaviour is consistent with the literature for subcritical flow at Re-10^3, where vortex shedding persists but becomes three-dimensional and turbulent, resulting in less organised wake structures in 2D simulations [18].

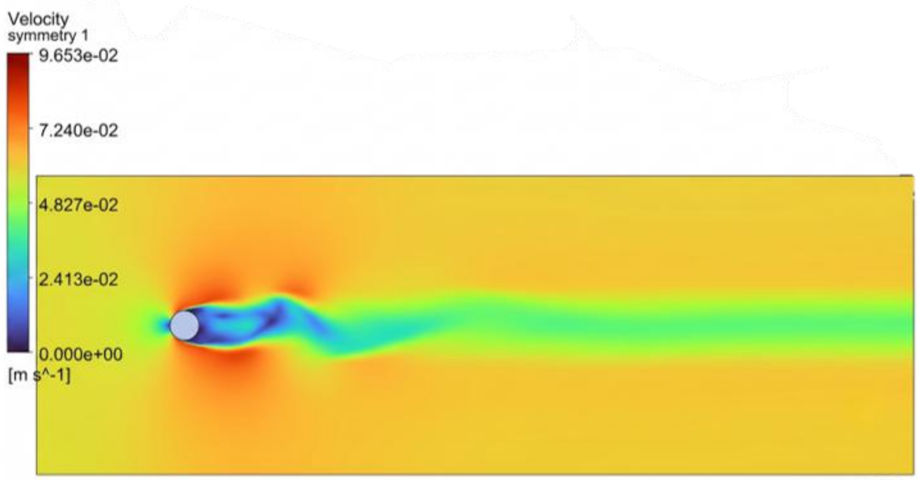

Figure 4. Velocity magnitude contour for Re = 4000 (Turbulent Wake). A wide, diffuse wake is observed with reduced coherence of vortex structures. Max velocity: 9.653×10^{-2} m/s

2.4. Comparative Analysis

Table 3 presents a comparative summary of the key flow parameters across the three simulated Reynolds numbers. The progressive transition in wake behaviour is clearly captured: from a completely steady symmetric wake (Re = 20), through a periodic, well-organised Von-Kármán vortex street (Re = 200), to a broader turbulent wake with reduced vortex coherence (Re = 4000).

The Strouhal number is not applicable at Re = 20 due to the absence of vortex shedding. At Re = 200, St = 0.19 is in excellent agreement with the Williamson [3] correlation and the experimental data of Wieselsberger [20]. At Re = 4000, the Strouhal number approaches the near-constant value of St ≈ 0.20 that is broadly maintained throughout the turbulent subcritical regime. The maximum velocity ratio (U_max/U∞) increases from 1.29 at Re = 20 to 1.64 at Re = 4000, reflecting the increasing flow kinetic energy and the growing importance of inertial effects over viscosity.

Table 3. Comparative summary of flow characteristics at three Reynolds numbers

Re	Flow Regime	Strouhal No. (St)	Wake Structure	Max Velocity (m/s)
20	Laminar (Steady)	N/A	Symmetric, attached wake, no shedding	3.796×10^{-4}
200	Transitional (Shedding)	0.19	Periodic alternating Von-Kármán vortex street	4.374×10^{-3}
4000	Turbulent	0.20	Wide, diffused turbulent wake	9.653×10^{-2}

The results are in good qualitative agreement with the established flow regime map of Zdravkovich [18] and the numerical benchmarks of Braza et al. [16]. Minor quantitative discrepancies between the CFD results and published data are attributed to the two-dimensional assumption, which precludes three-dimensional instabilities that arise in practice even at moderate Reynolds numbers. Additionally, the finite domain height (5D) may introduce mild blockage effects, particularly at Re = 200 where the vortex street spreads transversely.

4. CONCLUSIONS

This study has successfully demonstrated the evolution of flow dynamics past a 2D circular cylinder across three Reynolds number regimes using ANSYS Fluent 2026 R1 CFD simulations. At Re = 20, the flow exhibits a completely steady, symmetric wake with two attached recirculation vortices and no vortex shedding, in agreement with the expected laminar regime for Re < 47. At Re = 200, a fully developed, periodic Von-Kármán vortex street is established. The estimated Strouhal number (St = 0.19) agrees well with the Williamson empirical correlation and published experimental benchmarks. At Re = 4000, the k-ω SST turbulence model captures a broad, diffuse turbulent wake with reduced vortex coherence, consistent with the subcritical turbulent regime. The grid independence test confirmed that the selected medium mesh provides numerically converged results with less than 1% deviation in drag coefficient compared to the fine mesh. The CFD methodology employed in this study demonstrates that ANSYS Fluent is an effective and reliable tool for investigating internal and external flow dynamics across a wide range of Reynolds numbers. Future work should consider three-dimensional simulations to capture spanwise instabilities, a finer parametric sweep of Reynolds numbers to more precisely identify transition boundaries, and a more detailed analysis of pressure coefficient distribution and drag/lift time histories.

ACKNOWLEDGEMENTS

This research was conducted as part of the coursework for BDI 41203 Computational Fluid Dynamics at the Faculty of Mechanical and Manufacturing Engineering, Universiti Tun Hussein Onn Malaysia. The author would like to thank the course instructor for guidance and ANSYS Inc. for the student license used in this study.

REFERENCES

[1] Kreith F, editor. Fluid mechanics. CRC press; 1999 Nov 29.

[2] Von Karman T. Über den Mechanismus des Widerstandes, den ein bewegter Körper in einer Flüssigkeit erfährt. Nachrichten von der Gesellschaft der Wissenschaften zu Göttingen, Mathematisch-Physikalische Klasse. 1911;1911:509-17.

[3] Williamson CH. Defining a universal and continuous Strouhal–Reynolds number relationship for the laminar vortex shedding of a circular cylinder. The Physics of fluids. 1988 Oct 1;31(10):2742-4. https://doi.org/10.1063/1.866978

[4] Sarpkaya T. A critical review of the intrinsic nature of vortex-induced vibrations. Journal of fluids and structures. 2004 May 1;19(4):389-447. https://doi.org/10.1016/j.jfluidstructs.2004.02.005

[5] Blevins RD. Flow-induced vibration. New York. 1977.

[6] Middleton WD. In the Wake of Tacoma: Suspension Bridges and the Quest for Aerodynamic Stability. Technology and Culture. 2003;44(3):618-20. https://doi.org/10.1353/tech.2003.0121

[7] Norberg C. Fluctuating lift on a circular cylinder: review and new measurements. Journal of Fluids and Structures. 2003 Jan 1;17(1):57-96. https://doi.org/10.1016/S0889-9746(02)00099-3

[8] Berger E, Wille R. Periodic flow phenomena. Annual Review of Fluid Mechanics. 1972 Jan;4(1):313-40. https://doi.org/10.1146/annurev.fl.04.010172.001525

[9] Roshko A. On the development of turbulent wakes from vortex streets. 1954 Jan 1. https://ntrs.nasa.gov/api/citations/19930092207/downloads/19930092207.pdf

[10] Henderson RD. Nonlinear dynamics and pattern formation in turbulent wake transition. Journal of fluid mechanics. 1997 Dec;352:65-112. https://doi.org/10.1017/S0022112097007465

[11] Barkley D, Henderson RD. Three-dimensional Floquet stability analysis of the wake of a circular cylinder. Journal of Fluid Mechanics. 1996 Sep;322:215-41. https://doi.org/10.1017/S0022112096002777

[12] Lourenco LM. Characteristics of the plane turbulent near wake of a circular cylinder. A particle image velocimetry study. 1993.

[13] Travin A, Shur M, Strelets M, Spalart P. Detached-eddy simulations past a circular cylinder. Flow, turbulence and combustion. 2000 Jan;63(1):293-313. https://doi.org/10.1023/A:1009901401183

[14] Beaudan PB. Numerical experiments on the flow past a circular cylinder at sub-critical Reynolds number. Stanford University; 1995.

[15] Jiang H, Cheng L. Strouhal–Reynolds number relationship for flow past a circular cylinder. Journal of Fluid Mechanics. 2017 Dec;832:170-88. https://doi.org/10.1017/jfm.2017.685

[16] Braza M, Chassaing PH, Minh HH. Numerical study and physical analysis of the pressure and velocity fields in the near wake of a circular cylinder. Journal of fluid mechanics. 1986 Apr;165:79-130. https://doi.org/10.1017/S0022112086003014